Unstable regimes for a Bose-Einstein condensate in an optical lattice

L. De Sarlo,* L. Fallani, J. E. Lye, M. Modugno,† R. Saers,‡ C. Fort, and M. Inguscio

LENS, Dipartimento di Fisica, and INFM, Università di Firenze via Nello Carrara 1, I-50019 Sesto Fiorentino (FI), Italy

We report on the experimental characterization of energetic and dynamical instability, two mechanisms responsible for the breakdown of Bloch waves in a Bose-Einstein condensate interacting with a one-dimensional (1D) optical lattice. A clear separation of these two regimes is obtained by performing measurements at different temperatures of the atomic sample. The time scales of the two processes have been determined by measuring the losses induced in the condensate. A simple phenomenological model is introduced for energetic instability while a full comparison is made between the experiment and the 3D Gross-Pitaevskii theory that accounts for dynamical instability.

PACS number(s): 03.75.Kk, 03.75.Lm, 32.80.Pj, 05.45.−a

I. INTRODUCTION

The interest in the system made by neutral atoms in optical lattices has constantly been growing in recent decades since the development of efficient laser-cooling techniques, which opened the possibility of observing quantum effects on the motion of atomic ensembles. The physics of quantum particles in periodic potentials can be described in terms of Bloch waves [1] and indeed many effects originally predicted for electrons in a lattice of ions have been observed for ultracold thermal atoms moving in optical lattices [2] and, more recently, in quantum degenerate samples with the observation of long-lived Bloch oscillations in a degenerate Fermi gas [3]. In particular, the achievement of Bose-Einstein condensation (BEC) in dilute atomic gases has allowed the possibility to repeat these experiments with ensembles of particles all occupying the same Bloch state, in principle enhancing the visibility of these quantum effects [4–7]. However, when the density of the sample increases, as in the case of a trapped condensate, interactions among the atoms forming the BEC may significantly change the simple single-particle picture. The interaction-induced nonlinearity is responsible for the observation of many other phenomena, notably the phase transition from a superfluid to a Mott insulator [8] and the generation of bright gap solitons [9]. Furthermore, it can be shown that there exists a range of parameters for which nonlinearity makes the Bloch-like solutions of the wave equation describing the system unstable.

In this paper we report on the experimental characterization of the unstable regimes for a BEC in a one-dimensional (1D) optical lattice, obtained through a clear measurement of the time scales describing the evolution of the system, in remarkable agreement with the theory.

The phenomenon of instability of a BEC in a 1D optical lattice has already been the subject of experimental [10–13]

and theoretical [14–22] work. In particular, in the framework of the Gross-Pitaevskii (GP) theory in a periodic potential, there are different mechanisms responsible for the breakdown of the initial superfluid state. On one hand, as demonstrated by Landau in the context of superfluid helium [23], there is a critical velocity (related to the sound velocity of the system) beyond which the system can lower its energy by emitting phononlike excitations which deplete the original state. This kind of instability, which is closely related to the energy spectrum of the system, is called *energetic instability* and it has been observed for a harmonically trapped condensate in [24]. On the other hand, due to the interplay between nonlinearity and periodicity in the GP equation governing the dynamics of the system, for certain values of lattice height and velocity an arbitrarily small fluctuation of the original state may grow exponentially in time, thus destroying the initial Bloch state. This kind of instability, common to many nonlinear systems in a periodic potential, is usually called *dynamical* or *modulational instability* since it is connected to the dynamic equation which describes the system. In Fig. 1 we show a schematic diagram of the stability of the first band of Bloch states for a condensate in a 1D optical lattice as a
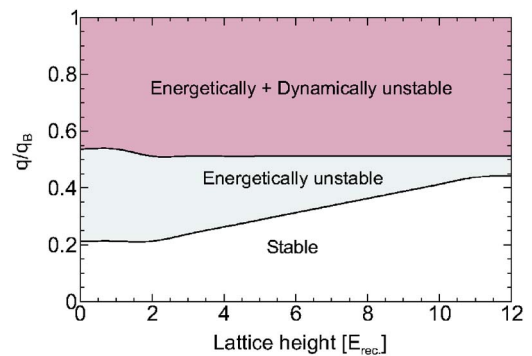
FIG. 1. (Color online) Schematic plot of the stability of Bloch matter waves in the first band of a 1D optical lattice: white area corresponds to the stable region, in the light gray area the condensate is energetically unstable, and in the dark gray area it is both energetically and dynamically unstable [14,21]. Vertical axis is the Bloch quasimomentum q and horizontal axis is the lattice height in recoil energy (see Sec. II).

---

*Electronic address: desarlo@lens.unifi.it

†Also at BEC-INFM Center, Università di Trento, I-38050 Povo (TN), Italy.

‡Present address: Department of Physics, Umeå University, S-901 87 Umeå, Sweden.

013603-1

function of the lattice height. The theory predicts the existence of three regions depending on the the condensate quasimomentum q, corresponding to a regime where Bloch waves are stable solutions, or they are energetically unstable, or they are both energetically and dynamically unstable.

Although the distinction of these two mechanisms is straightforward from the theoretical point of view, in the experiments it is much more difficult to separate energetic and dynamical instability since, no matter which is the mechanism responsible for the onset of instability, the original BEC superfluidity will be compromised and losses of atoms in the ground state are expected. Furthermore, as it is shown in Fig. 1, the stability of the system depends on the height of the optical lattice: when the lattice height is greater than the chemical potential of the BEC, the so-called tight-binding regime (lattice height greater than $5E_{rec}$ in Fig. 1), energetic instability is only a narrow boundary between the regions of stability and dynamical instability. On the other hand, when the lattice is weak compared to the chemical potential, as in the experiments reported in this paper, there is a wide range of values of quasimomentum for which the system is energetically but not dynamically unstable. The lack of control over the condensate quasimomentum in the very first experiment devoted to this subject made the separate identification of the two regimes a very difficult task [10]. The excitation of the collective dipole mode in the combined (harmonic plus periodic) potential used in [10,11] can indeed demonstrate the onset of instability but cannot easily discriminate between different mechanisms because, during a single experimental run, the condensate velocity (and therefore its quasimomentum) evolves throughout the first band and thus explores both regimes (see Fig. 1). Actually the phenomena observed in [10] were attributed to energetic instability because the 1D Gross-Pitaevskii theory used to analyze the data cannot reproduce some of the observed experimental features. This in turn suggested that finite-temperature effects could play a role. However a comparison with the full 3D theory shows that the dynamics observed in [10] can be fully understood in terms of dynamical instability [21].

In the present paper we show that the precise control of the BEC quasimomentum, obtained using an optical lattice moving at constant velocity, is crucial to distinguish the different unstable regimes. The experimental procedure implemented in this work allows a comparison with the predictions of the theory and a study of the stability of the condensate also in the excited bands of the periodic potential [13]. The structure of the paper is the following. In Sec. II we describe the experimental setup, in Sec. III we present our results obtained for energetic instability and discuss the role of thermal excitations, and then in Sec. IV we present a comprehensive investigation of the phenomenon of dynamical instability and show that it is possible to clearly distinguish it from energetic instability. In the Appendix we discuss the effect of the harmonic trapping potential on the dynamics of the BEC adiabatically loaded in the moving optical lattice.

II. EXPERIMENTAL SETUP AND PROCEDURE

We produce a BEC of ^{87}Rb atoms in the hyperfine state $|F=1;m_F=-1\rangle$ using a standard double magneto-optical trap

(MOT) apparatus. Our condensate typically contains 3×10^5 atoms and it is produced by radio-frequency-induced evaporation of the atomic sample confined in an elongated magnetic harmonic trap characterized by an axial and radial frequency of $\omega_z=2\pi\times(8.74\pm0.03)$ Hz and $\omega_\perp=2\pi \times(85\pm1)$ Hz, respectively. The 1D optical lattice is formed by two counterpropagating laser beams obtained from a Ti:sapphire source and it is aligned along the axis of the magnetic trap. The interference profile has a spatial period of $\lambda/2$, where $\lambda\simeq820$ nm is the wavelength of the laser. Using two single-mode fibers we obtain two Gaussian beams with a radius of 200 μm, much larger than the condensate radial size. In this paper we report measurements carried out with lattice heights of $s=0.2$ and 1.15, where s is the height of the optical potential in recoil energies [$E_{rec}=h^2/(2\lambda^2m)$, m being the mass of a Rb atom]. The lattice height is calibrated via Bragg scattering of the condensate and is monitored throughout the experiment [25]. The frequencies of the two beams are controlled independently by two acousto-optic modulators which use the same time base. This allows us to precisely control the velocity of the lattice v_L, which is related to the frequency difference between the two beams, $\Delta\nu$, by the following relation:

$$v_L = \frac{\lambda}{2}\Delta\nu. \tag{1}$$

In the laboratory frame the lattice potential can be written as

$$V_L(z) = sE_{rec}\cos^2\left(\frac{2\pi(z-v_Lt)}{\lambda}\right) \tag{2}$$

while the confining magnetic potential is

$$V_{HO}(\mathbf{x}) = \frac{1}{2}m(\omega_\perp^2 r^2 + \omega_z^2 z^2). \tag{3}$$

After producing the condensate in the harmonic potential, we load it adiabatically into a single Bloch state ramping the intensity of the lattice from zero to its final value in a time $t_R\simeq2$ ms. During the ramp time the lattice velocity is kept constant and no acceleration is used. This process can be viewed as a deformation of the spectrum of the system from a free-particle one (i.e., parabolic) to a Bloch one, in which the states are labeled by a band index n and a quasimomentum q (which has the periodicity of the reciprocal lattice, $2q_B=4\pi/\lambda=2mv_B/\hbar$). If the ramping time is sufficiently long so that this deformation can be considered adiabatic, the condensate is transferred to a Bloch state with quasimomentum $q=|v_L|m/h$, belonging to the first band if $|v_L|<v_B$, to the second band if $v_B<|v_L|<2v_B$, and to the nth band if $(n-1)v_B<|v_L|<nv_B$ [4,5] (further details are given in the Appendix). To observe the effect of nonlinearity, we maintain a high density in the sample, keeping the harmonic trapping potential on during the whole experimental procedure. This is crucial to enter the regime where the effects of dynamical instability are observable.

In order to study the two mechanisms of instability we perform a time-resolved analysis of the losses in the condensate induced by the lattice for different values of quasimomentum, band index, and lattice height. The general proce-
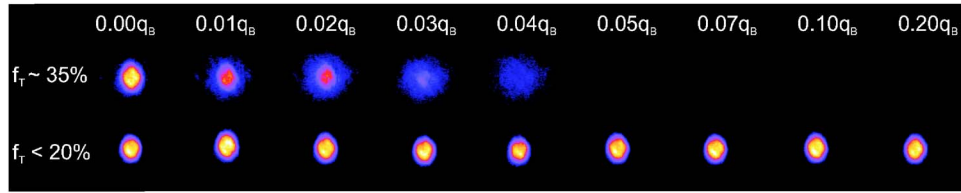
FIG. 2. (Color online) Absorption images of the condensate interacting for $t=15$ s with a lattice with $s=0.2$ for different values of quasimomentum ranging from 0 to $0.20q_B$ and for, respectively, a condensed fraction of about 65% (top) and no detectable thermal component (bottom).

dure is the following. After loading the condensate into a single Bloch state we let it interact with the moving lattice for a time t, then we switch off adiabatically the lattice, release the atoms from the magnetic trap, and measure the number of atoms remaining in the condensate by taking an absorption image along the radial direction after 28 ms of expansion. This allows us to reconstruct the evolution of the number of atoms as a function of time and to measure the lifetime of the condensate τ as a function of q. Without the optical lattice the BEC lifetime is limited to $\tau=23\pm3$ s by the heating due to current noise in the coils producing the magnetic trap. The introduction of a stationary lattice (i.e., a standing wave) introduces two further heating mechanisms: resonant photon scattering and lattice vibrations due to mechanical noise on the optics setting the path of the two beams. Using the Ti:sapphire laser at a wavelength of 820 nm (74 THz detuned from the $D1$ line) makes heating from resonant photon scattering completely negligible, while we measured that the second effect becomes dominant when the lattice height is higher than one recoil energy ($\tau=17\pm2$ s with $s=1.15$). In the case of a moving optical lattice this lifetime can be strongly reduced if instability mechanisms are activated.

In particular we found that, also for a very small velocity, the lifetime measurement is critically affected by the presence of a residual cloud of noncondensed atoms surrounding the BEC. Even a barely detectable fraction of thermal atoms can significantly shorten the lifetime of the condensate and thus the temperature of the system must be taken into account. For this reason, in order to control the temperature of the sample, the radio frequency used in evaporative cooling is kept on after the production of the BEC (rf shield).

III. THE ROLE OF THE THERMAL FRACTION: ENERGETIC INSTABILITY

The effect of a thermal fraction can be seen in Fig. 2. There we show two series of pictures taken at different lattice quasimomenta ranging from 0 to $0.2q_B$ and for two values of the final radio frequency used for the evaporation, corresponding to different temperatures of the atomic cloud. When we have an almost pure condensate (thermal fraction below 20%, limited by our imaging sensitivity), the number of atoms remaining after 15 s of interaction is not sensitive to the lattice velocity (bottom part of Fig. 2), while in the case of a mixed cloud (thermal fraction $\simeq35\%$) even a small velocity leads to a strong reduction in the number of atoms (top part of Fig. 2). Note that the velocities presented in these

pictures are well below the threshold for the onset of dynamical instability for the experimental parameters of Fig. 2 corresponding to $q\simeq0.5q_B$ (see Sec. IV); we will come back to this point at the end of this section. Clearly, the presence of a thermal cloud strongly affects the number of atoms remaining in the condensate after the interaction with the optical lattice. This effect can be connected to energetic instability which requires the presence of a dissipative mechanism: the thermal cloud provides a channel to absorb the excitations of the condensate and drive it toward a lower-energy state. When the thermal component is strongly depleted, the condensate experiences a better insulation from the environment and the effect of instability is less severe. Note that this process cannot be studied with the Gross-Pitaevskii equation which does not include any coupling with the thermal cloud.

In order to test this hypothesis quantitatively we have measured the number of atoms in the condensed fraction as a function of quasimomentum for three different times of BEC-lattice interaction, using a 35% thermal fraction. The results are shown in Fig. 3. As one can see, the number of atoms N slowly reduces with increasing q up to a critical quasimomentum q_0, after which it remains constant. The
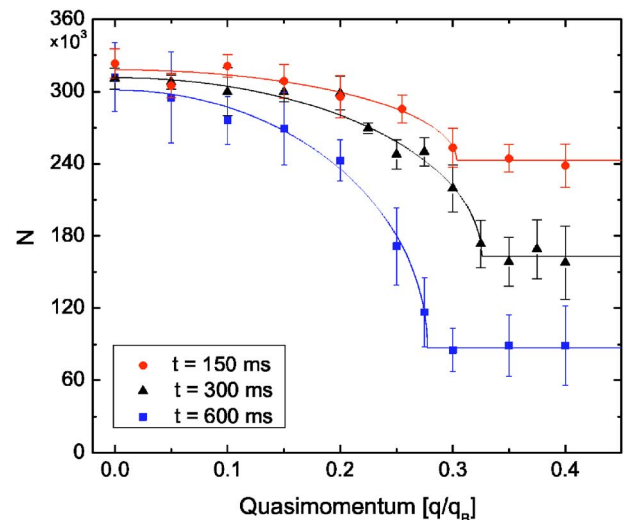
FIG. 3. (Color online) Number of atoms remaining in the condensate as a function of quasimomentum in a lattice with $s=0.2$ for different interaction times t. The three data sets refer, respectively, to $t=150$ (circles), 300 (triangles), and 600 ms (squares). The initial cloud has a condensed fraction of about 65%. The curves are fitted to experimental points using Eq. (9) with N_0, b, and q_0 as free parameters.

smooth behavior of N as a function of q below this critical value seems not to be compatible with the threshold process expected in [14]. However this behavior can be related to the inhomogeneity of the condensate with an argument similar to the one of Ref. [10]. As we already pointed out, the onset of energetic instability is related to the sound velocity within the condensate: once the center-of-mass velocity exceeds this value the system can lower its energy by emitting phononlike excitations associated with sound propagation along the axial direction. For an infinite cylindrical condensate this is a threshold process since the sound velocity, which depends on the density averaged over the radial direction, takes a finite value. In particular, in the radial Thomas-Fermi regime it can be expressed as [26]

$$v_s = \sqrt{\frac{\tilde{g} n_0}{2 m^*}}, \qquad (4)$$

where $\tilde{g}$ is an effective interaction constant which takes into account the presence of the lattice, m^* is the effective mass for the condensate Bloch state, and $n_0/2$ is the radially averaged density expressed in terms of the peak density of the sample n_0. Assuming that a similar relation holds locally in an elongated condensate with peak density $n_0(z)$, we can argue that the condition for local energetic stability is $v_s(z) > v_{n,q}$ where $v_{n,q}$ is the Bloch velocity of the condensate loaded in band n with quasimomentum q and $v_s(z)$ is the sound velocity of a cylindrical condensate with peak density $n_0(z)$. As one can verify, for the values of quasimomentum and lattice height involved in these measurements, the Bloch dispersion is only slightly different from the free-particle one for which $v_{n,q} = \hbar q/m$, and it is correct to assume $\tilde{g} = g = 4\pi\hbar^2 a_s/m$ and $m^* = m$, where m is the mass of a rubidium atom and a_s is the s-wave scattering length. The above condition for energetic stability can be recast as

$$n_0(z) > \frac{2\hbar^2 q^2}{gm} = Cq^2 \qquad (5)$$

where we indicate with $n_0(z)$ the density of the condensate along its axis. One can therefore obtain the fraction of the condensate that is energetically stable by integrating the density over the region satisfying Eq. (5),

$$f_{q_0}(q) = \frac{1}{N_0} \int_{n_0 > Cq^2} dz \int\int dx\, dy\, n(\mathbf{r}), \qquad (6)$$

where N_0 is the number of atoms in the condensate and $n(\mathbf{r})$ its density distribution.

In our experiments the lattice produces a weak modification of the density profile. It is therefore correct to assume as local density (i.e., averaged over the lattice spacing) the Thomas-Fermi profile of the condensate in the magnetic potential,

$$n(x,y,z) = \frac{\mu}{g}\left(1 - \frac{x^2 + y^2}{R_\perp^2} - \frac{z^2}{R_z^2}\right), \qquad (7)$$

where μ is the chemical potential of the condensate. This gives the fraction of the condensate which is energetically stable,

$$f_{q_0}(q) = \sqrt{1 - \left(\frac{q}{q_0}\right)^2}\left[1 + \frac{1}{2}\left(\frac{q}{q_0}\right)^2 + \frac{3}{8}\left(\frac{q}{q_0}\right)^4\right]$$
$$\times\, \theta\left(1 - \left|\frac{q}{q_0}\right|\right), \qquad (8)$$

where $\theta(x)$ is the Heaviside function and $q_0 = \sqrt{(\mu m)/(2\hbar^2)}$ is the threshold value for energetic instability in a homogeneous cylindrical condensate with peak density n_0, namely, the quasimomentum for which Eq. (5) cannot be satisfied for any z. The value of q_0 can be theoretically calculated also beyond the approximation of free-particle dispersion and is independent of the BEC-lattice interaction time provided that the density is not significantly reduced by the losses induced by the instability. As shown in Fig. 2, this simple assumption is not correct for long interaction times: as the condensate loses atoms it becomes less dense and therefore more unstable because q_0 tends to zero. However, since the sound velocity scales with $N^{1/5}$, it changes only slightly even for a strong reduction of N and the assumption of treating q_0 as
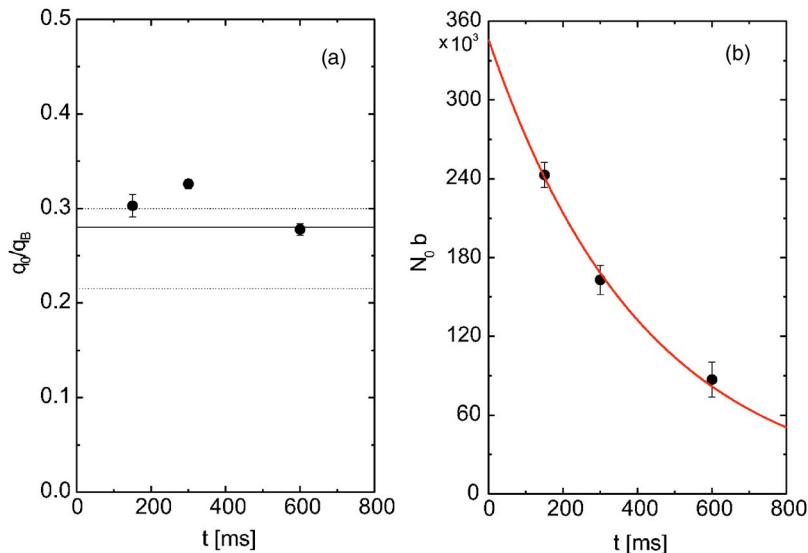
FIG. 4. (Color online) (a) Fitted values for q_0 at different interaction times (symbols) and theoretical prediction for a homogeneous cylindrical condensate with the same experimental parameters (solid line). Dashed lines mark the error on the theoretical value which is due to uncertainty in the measured peak density of the sample. (b) Number of atoms above q_0 given by the product $N_0 b$ obtained from the fit to the experimental data as a function of interaction time t: continuous line is a fit to an exponential decay from which we measure a characteristic time of $\tau_{EI} = 416 \pm 55$ ms.
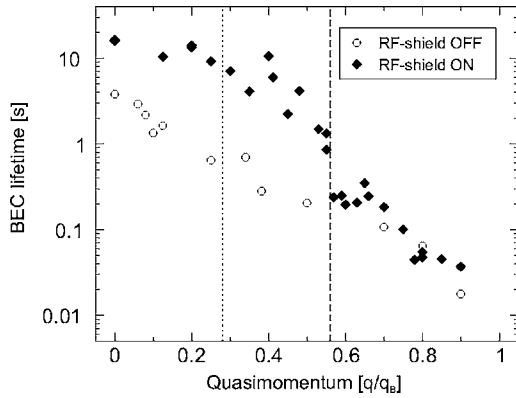
FIG. 5. Lifetime of the condensate with and without rf shield as a function of quasimomentum for the first Bloch band (logarithmic plot). The lattice height is $s=0.2$ and vertical lines are drawn in correspondence of the calculated thresholds for a homogeneous cylindrical condensate respectively for energetic (dotted) and dynamical (dashed) instability [21]. Error bars are smaller than point size.

constant in time; we will come back to this point when discussing our experimental results.

In order to derive a simple expression for N as a function of q and t one has to make some further assumptions on the decay induced by energetic instability. We assume that for a given q the number of atoms in the stable fraction [i.e., $N_0 f_{q_0}(q)$] is constant in time, while the number of atoms initially in the unstable fraction (i.e., $N_0[1-f_{q_0}(q)]$) decays with a time behavior $b(t)$. We thus obtain for N the following expression:

$$N(q,t) = N_0 f_{q_0}(q) + b(t)N_0[1-f_{q_0}(q)]. \qquad (9)$$

Note that $N_0 b(t)$ can also be viewed as the number of atoms remaining in the condensate after a time t, once it is entirely unstable ($f_{q_0}=0$) and N no longer depends on q. Note also that we do not make any assumption on the explicit form of $b(t)$, which, for a given time t, enters Eq. (9) only as a parameter. In principle one could think that, as atoms are removed from the unstable fraction, some of the atoms in the stable fraction are transferred to the unstable part in order to *refill* the losses: this case would correspond to considering N_0 as time dependent in Eq. (9).

The lines shown in Fig. 3 are a fit of Eq. (9) to the experimental data taken for three different values of t with N_0, b, and q_0 as free parameters. As one can see, our simple model reproduces the experimental points very well within the error bars, which are taken as the standard deviation of a five-measurement average; in particular, as one can see looking at the values of the fitted functions at $q=0$, N_0 does not significantly depend on time. In Fig. 4(a) we report the values of q_0 obtained from the fits shown in Fig. 3 together with the theoretical prediction obtained for a homogeneous cylindrical condensate. As expected, the measured values of q_0 do not exhibit a significant dependence on the BEC-lattice interaction time t [see Fig. 4(a)]. Notice that throughout the measurement the number of atoms is reduced at most by a factor of 1.62 which corresponds to a change in the sound velocity of around 20%. This is comparable with our uncer-
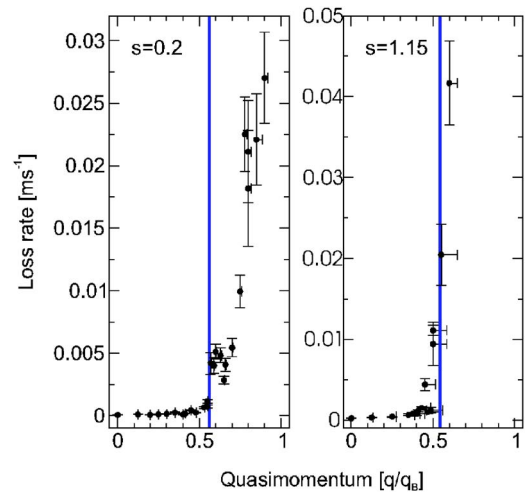
FIG. 6. (Color online) Measured loss rate of the BEC (reciprocal of lifetime) as a function of quasimomentum in the first Bloch band with $s=0.2$ and 1.15, respectively. The vertical lines correspond to the theoretical values for the threshold of dynamical instability [21]. The horizontal error bar is due to the presence of the confining harmonic potential as explained in the Appendix.

tainty in the measurement of the density and with the spread of the values of q_0 extracted from the fits. We can directly compare these values with the theoretical prediction for the threshold of energetic instability for a homogeneous cylindrical condensate [21]. Given our uncertainty on the density of the sample, which propagates into the theoretical calculations, the agreement between theory and experiment is good. Furthermore one can extract an estimate for the characteristic time of energetic instability by looking at the decay of the number of atoms above threshold $b(t)$. Assuming for b an exponential decay (i.e., $b=b_0 e^{-t/\tau_{EI}}$) the time scale for energetic instability for the experimental condition of Fig. 3 is $\tau_{EI} \sim 400$ ms, as shown in Fig. 4(b). Due to the experimental difficulties in controlling the thermal fraction of the initial atomic cloud, we did not study the dependence of τ_{EI} on the condensed fraction. This would be a very interesting measurement since it could provide a further insight into the role of the thermal fraction; by the same token a more accurate determination of N_0 and q_0 could allow the investigation of the transfer of atoms from the stable to the unstable fraction which is ultimately responsible for the complete destruction of the condensate. However, as we pointed out in the description of Fig. 2, as the condensed fraction increases the number of atoms remaining in the condensate after a fixed t increases as well.

These results demonstrate that a thermal fraction triggers the dissipative mechanism connected with energetic instability and therefore it is possible to strongly reduce this dissipation using a radio-frequency shield in order to make the measurement with no discernible thermal fraction. This is particularly important if we want to separately address the two regimes of energetic and dynamical instability. The results of this procedure are shown in Fig. 5 where we plot the BEC lifetime as a function of quasimomentum for $s=0.2$ with and without rf shield. Without the use of a rf shield (open circles) it is impossible to distinguish the onset of
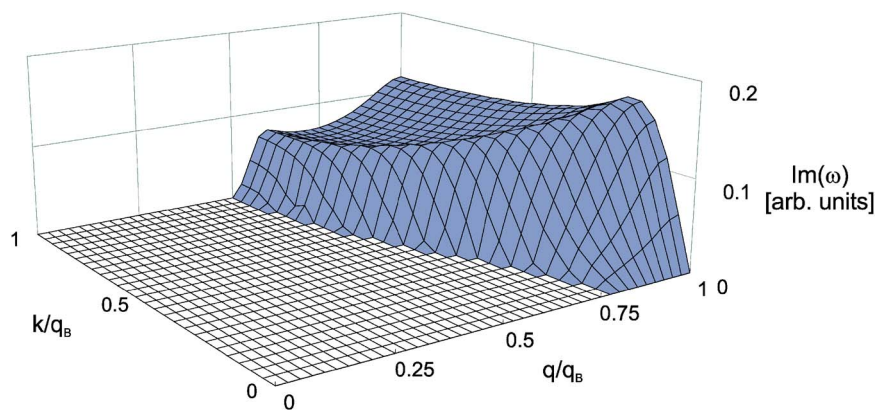
FIG. 7. (Color online) Calculated growth rates $|\text{Im}(\omega)|$ of the excitation modes of an infinite cylindrical condensate in a periodic lattice with $s=1.15$, as a function of the condensate and excitation quasimomenta q and k, respectively (first Bloch band).

dynamical instability at $q=0.56q_B$ because this feature is masked by the reduction of the number of atoms caused by energetic instability. On the other hand, by keeping an almost pure condensate throughout the experiment (filled diamonds in Fig. 5) the discontinuity in the lifetime entering the dynamically unstable regime becomes clearly visible despite a residual reduction of the lifetime due to noncomplete efficiency of the rf shield. An important point is that, even though without a rf shield there is no measurable threshold, the lifetime deep in the dynamically unstable regime is the same with or without the rf shield as dynamical instability is the dominant loss mechanism in both cases. We will show in the next section, devoted to a deep experimental investigation of this regime, that indeed dynamical instability takes place much faster than energetic instability. We note here that, as already well established in literature [27], the introduction of a rf shield increases the lifetime even in the absence of the optical lattice and this explains the difference in the measured lifetime at $q=0$.

IV. "ZERO-TEMPERATURE" MEASUREMENTS: DYNAMICAL INSTABILITY

For $q>0.5q_B$ we observed the onset of dynamical instability characterized by two distinct signatures which we will discuss in some detail: a threshold value of quasimomentum above which the lifetime dramatically decreases (as pointed out above) and, for higher values of quasimomentum, the presence of complex structures in the density distribution of the expanded atomic cloud [13].

In Fig. 6 we plot the reciprocal of the lifetime of the condensate (loss rate) as a function of quasimomentum in the first Bloch band for two different values of lattice height. For both values of s we observe a precise value of quasimomentum for which there is a sudden increase in the loss rate of atoms from the BEC. For our experimental parameters, this threshold is almost independent of the condensate density so that, differently from the case of energetic instability, inhomogeneity does not play a significant role in this context. Indeed there is a remarkable agreement between the experiment and the calculated thresholds for a homogeneous cylindrical condensate shown in Fig. 6 as vertical lines.

From a theoretical point of view the onset of dynamical instability is signaled by the appearance of excitations of

definite wave vector k, which grow exponentially in time, thus modifying the momentum distribution of the system characterized by peaks spaced by the periodicity of the lattice in the reciprocal space, $2q_B$ [4,28]. The character of these excitation modes can be obtained by considering small deviations from the condensate wave function and solving the corresponding Bogoliubov equations, as discussed in [14,29] for the 1D case and in [21] for a 3D system. For the
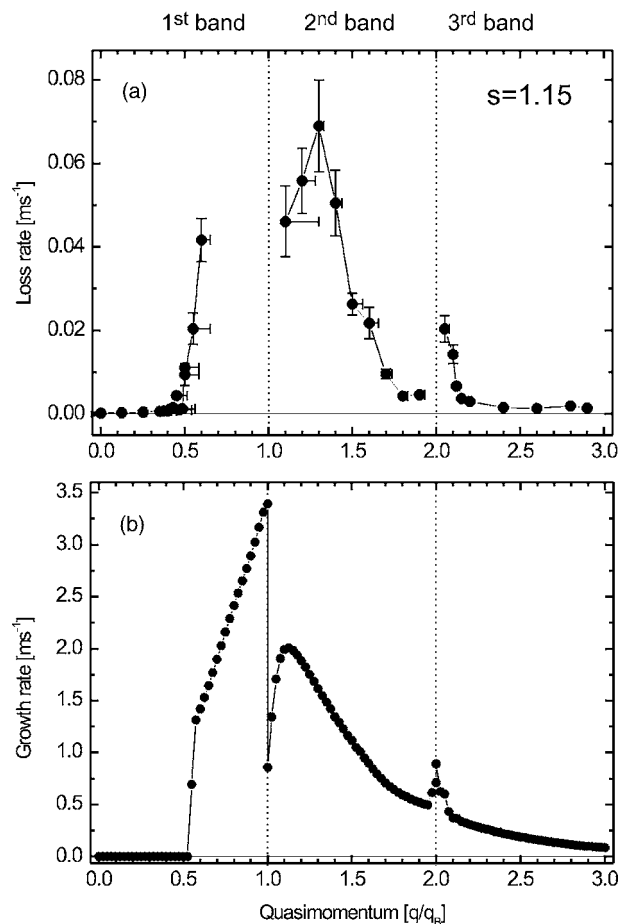
FIG. 8. Comparison between the measured loss rates of atoms from the condensate (reciprocal of lifetime) and the theoretically calculated growth rates of the most unstable modes in the linear regime. Lattice height is $s=1.15$. Note that the measurements span the first three Bloch bands.
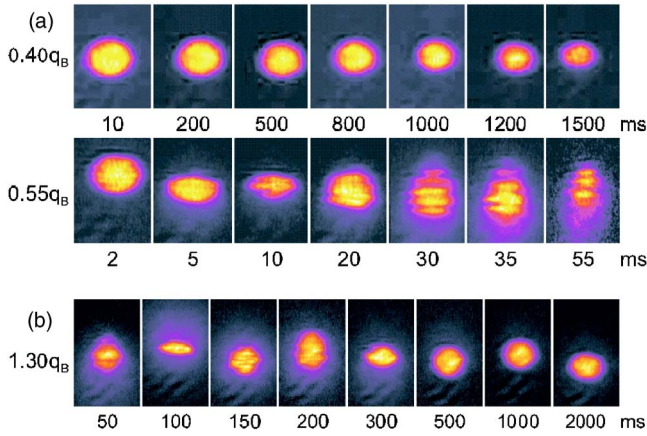
FIG. 9. (Color online) (a) Absorption images of the expanded condensate after different interaction times with a lattice with $s=1.15$ for two different values of quasimomentum. Note the sudden change of time scale crossing the threshold of dynamical instability at $q=0.525q_B$ and the appearance of structures in the density profiles for the unstable case ($q=0.55q_B$). (b) Reabsorption of excitations following 5 ms of interaction with the lattice and different times of evolution in the pure harmonic potential after switching off the lattice. In all these pictures the lattice moves from top to bottom.

system considered in this work when $q \gtrsim 0.5q_B$, the frequency of some modes in the excitation spectrum develops a nonzero imaginary part $\text{Im}(\omega)$ (see Fig. 7), which is the distinctive feature of dynamical instability and corresponds to the fact that, once excited, these modes will grow exponentially in time. As is shown in Fig. 7, for a given value of q there exists a range of such unstable wave vectors k, which is more and more extended as q approaches the band edge. Among all these unstable modes the one with the highest growth rate plays a major role in the dynamics of the unstable condensate.

The unambiguous attribution of the observations to the phenomenon of dynamical instability has been possible by comparing the measured loss rates (inverse of the lifetime) to the calculated growth rates of the most dynamically unstable modes. The results of this comparison are shown in Fig. 8 for a lattice with $s=1.15$. We point out that a full quantitative comparison between theory and experiment cannot be performed because the measurements occur outside the validity of the linear analysis on which the theory is based. However, the distinctive agreement between the theory and the experiment indeed shows that the observed phenomenon is dynamical instability and that the mode which is most unstable in the very initial stage of the dynamics (i.e., when linear theory is correct) imprints its time scale on the following dynamics.

For those quasimomenta for which dynamical instability is more severe and thus lifetimes are shorter, we observed the appearance of complex structures in the expanded density profiles, shown in Fig. 9 for $s=1.15$ and $q=0.55q_B$. These can be the signature either of a density modulation or a phase fragmentation that leads to the observed fringes through an interferencelike effect [30]. As already stated in [13] we have observed the disappearance of the fringes as the condensate reverts to its initial state if we let it evolve in the magnetic
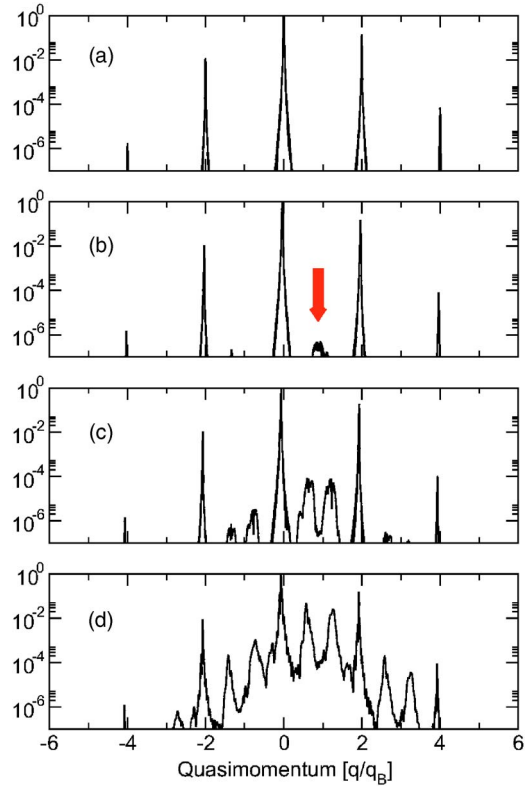
FIG. 10. (Color online) Calculated axial momentum distribution $P(p_z)$ of the condensate in the combined harmonic trap plus optical lattice for $t=12,33,48,51$ ms [from (a) to (d)] (logarithmic plot). The simulation is performed with $s=1.15$ and $v_L=0.55v_B$. The arrow in (b) marks the appearance of the unstable modes.

potential alone, after switching off the lattice. This process, however, takes place in a much longer time scale than the one of dynamical instability (lifetime can be of the order of a few milliseconds). In order to compare our observations with the theory, we have simulated the actual experimental procedure by solving the time-dependent 3D GP equation

$$i\hbar\frac{\partial}{\partial t}\Psi(\mathbf{x},t) = \left[-\frac{\hbar^2}{2m}\nabla^2 + V(\mathbf{x},t) + gN|\Psi|^2\right]\Psi(\mathbf{x},t),$$

(10)

where V is the sum of the harmonic (2) and periodic potentials (3). From the solution of Eq. (10) we extracted the axial power spectrum, defined as (the tilde indicates the Fourier transform along z) [20]

$$P(p_z) \equiv 2\pi \int r\,dr |\tilde{\Psi}(r,p_z)|^2$$

(11)

which is shown in Fig. 10. The upper frame [Fig. 10(a)] represents the momentum distribution at the end of the initial ramp, and is characterized by sharp peaks localized at integer multiples of $2q_B$ as discussed above. Then, in accordance with the prediction of the linear analysis, some modes of complex frequency start growing as indicated by the arrow in
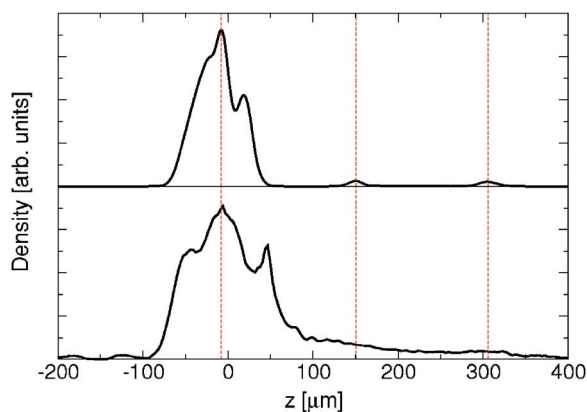
FIG. 11. (Color online) Comparison between the simulated ballistic expansion of the momentum distribution shown in Fig. 10(d) (top) and the cross section of the measured expanded density distribution of the condensate (bottom). In both cases the expansion time is 28 ms, $s=1.15$, $q=0.55q_B$, $t=50$ ms, and the lattice is adiabatically switched off, ramping down its intensity in 2 ms. Vertical lines mark the three main peaks of the calculated momentum distribution corresponding respectively to 0, $1.01\hbar q_B$, and $2\hbar q_B$. In both cases the lattice is moving in the direction of positive z.

FIG. 12. (Color online) Plot of the Bloch velocity as a function of quasimomentum in the first band for $s=1.15$. The dashed line is the free-particle velocity (i.e., $v=\hbar q/m$). Notice that the deviation of the Bloch velocity from the free-particle one increases as q increases.

Fig. 10(b) (in the numerical simulation these modes are triggered by the numerical noise). Afterward, the nonlinear dynamics introduces processes of mode mixing and the momentum distribution gets complicated [Figs. 10(c) and 10(d)]. However, the structure is still characterized by well-localized peaks close to q_B, and the position of the peaks still shows invariance under translation of $2q_B$. From these results it is possible to calculate the expanded density profile and thus make a direct comparison with the experimental observations. This comparison is shown in Fig. 11 for $s=1.15$, $q=0.55q_B$, $t_R=10$ ms, and $t=50$ ms. The simulation well reproduces the structure of the central peak observed in the experiment, but the naive expectation that the expanded density profile of the condensate would simply reflect the structure of the momentum spectrum is not correct. We note that indeed the occurrence of dynamical instability may lead to a rapid population of the noncondensate (thermal) fraction, whose behavior in the linear regime is governed exactly by the same Bogoliubov equations as for the semiclassical fluctuations of the condensate discussed so far [31,32]. This means that the Gross-Pitaevskii approach may fail when dynamical instability yields a strong depletion of the "coherent" condensed fraction. In order to account for this, one should include in the theory also the interaction between the condensate and noncondensate fractions, which may become macroscopically populated for later times [33]. The formation of a thermal component could strongly affect the expanded density distribution masking the momentum component populated by the interaction with the optical lattice. Actually the experimental density profile reported in Fig. 11 (bottom) shows a uniform tail on the right side of the main peak compatible with a thermal fraction dragged by the lattice.

V. CONCLUSION

We reported on the experimental observation of energetic and dynamical instability of a BEC in a moving 1D optical lattice. A clear separation of the two regimes is obtained by controlling the temperature of the system and adiabatically loading the condensate in a Bloch state with precise quasimomentum.
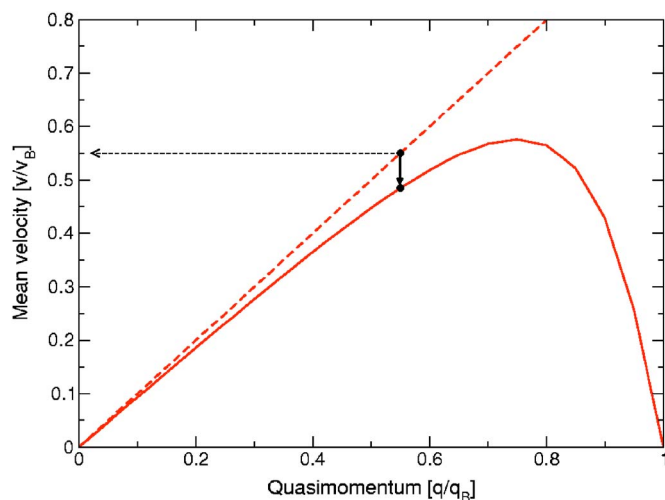
On one hand we have shown that energetic instability is deeply connected with the presence of a dissipative mechanism such as the one provided by thermal atoms around the condensate. We have derived a simple phenomenological model to take into account the effects of inhomogeneity of the atomic density distribution and found a good agreement between this model and the experiment. On the other hand we have observed that in the regime of dynamical instability the lifetime of the condensate is critically dependent on quasimomentum. We have compared this distinctive dependence of the condensate loss rate on quasimomentum with the theoretical prediction on the growth rate of unstable modes in the initial regime of the dynamics. We have found a very nice agreement thus demonstrating that the observed phenomenon is dynamical instability and that the initial excitations play a dominant role in the following evolution. Furthermore we compared the structure observed in the expanded density profile with the results of the solution of time-dependent 3D Gross-Pitaevskii equation finding a significant agreement between observation and theoretical calculation. We have been able to make a direct comparison between the timescales of the mechanisms of instability: we have experimentally demonstrated that in the regime of low lattice height and for a mostly condensed cloud, dynamical instability is one order of magnitude faster than energetic instability. Finally we note that the critical effect of a thermal cloud on the lifetime of the condensate in the presence of energetic instability suggests that it is possible to use a moving optical lattice to detect the presence of a noncondensed fraction well beyond the sensitivity of the imaging system usually employed in this field.
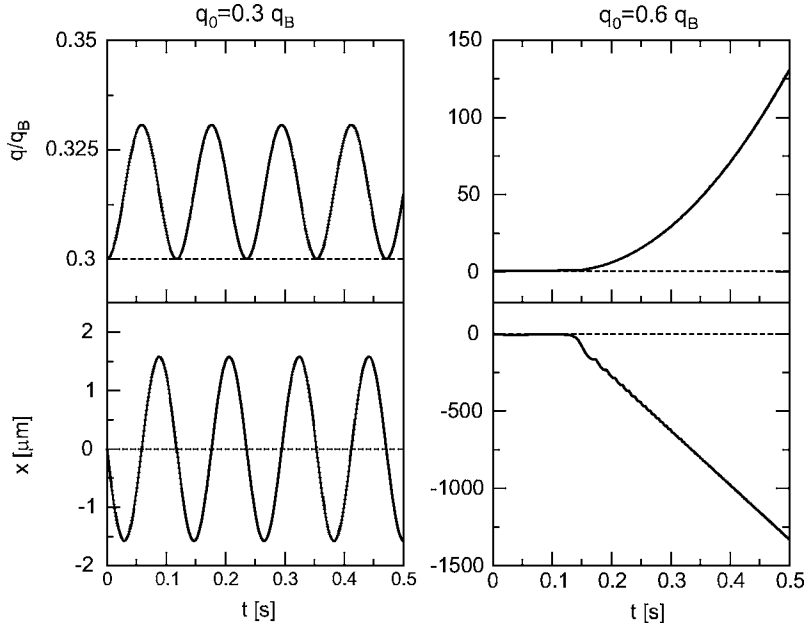
FIG. 13. Time evolution of a Bloch wave packet calculated from semiclassical Eq. (A1) for $s = 1.15$ and two different quasimomenta $q_0 = 0.3q_B$ and $0.6q_B$.

APPENDIX: THE EFFECT OF THE HARMONIC POTENTIAL

As explained in Sec. II, the adiabatic loading of the condensate in a moving optical lattice can be viewed as a slow transformation of the spectrum of the system from the free-particle parabola to a Bloch band. During this procedure the wave packet changes from that of a free particle to that of a Bloch state characterized by a velocity which is related to the energy spectrum by the well-known relation $v_{n,q} = \hbar^{-1}\partial_q E_{n,q}$, where $E_{n,q}$ is the energy of the eigenstate with quasimomentum q in band n. As is shown in Fig. 12 the difference between $v_{n,q}$ and the free-particle velocity increases with increasing q. Since the loading procedure conserves q, this means that the condensate acquires a finite velocity in the laboratory frame and starts moving in the harmonic potential. The center-of-mass motion in the frame of the laboratory follows the semiclassical laws of motion for a Bloch wave packet in an external force field [34]

$$\dot{z} = v_{n,q} - v_L = v_{n,q} - \hbar q_0/m,$$

$$\hbar \dot{q} = F, \qquad (A1)$$

where z is the direction of the lattice, m is the mass of a Rb atom, q_0 is the initial quasimomentum at which the conden-

sate is loaded, and F is the external force acting on the atoms. In our case this is the harmonic restoring force $F = -m\omega_z^2 z$. For low values of q, where the band has a parabolic shape (i.e., $E_{n,q} = \hbar^2 q^2/2m^*$), Eqs. (A1) can be analytically solved, leading to

$$z(t) = -\sqrt{\frac{m^*}{m}}\frac{v_0}{\omega_z}\sin\left(\sqrt{\frac{m}{m^*}}\omega_z t\right),$$

$$q(t) = q_0 + \frac{m^* v_0}{\hbar}\left[1 - \cos\left(\sqrt{\frac{m}{m^*}}\omega_z t\right)\right], \qquad (A2)$$

where $v_0 = \hbar q_0(1/m^* - 1/m)$. This solution is an oscillation in both real and quasimomentum space at the trap frequency rescaled by the effective mass $m^* = \hbar(\partial_q v_{n,q})^{-1}$. The amplitude of this oscillation in real space (~ 1 μm) is too small to be measured by our imaging system while the amplitude of oscillation in momentum space cannot be neglected. Increasing q, when the parabolic approximation of the band fails Eqs. (A1) can be still integrated giving asymmetric oscillations. Eventually, as shown in Fig. 13, for sufficiently high values of q, the solution of Eqs. (A1) ceases to be oscillatory: the condensate motion becomes unbounded and quasimomentum indefinitely grows. We took into account the motion of the Bloch wave packet in quasimomentum space considering an uncertainty on q for the data reported in Figs. 6 and 8 given by the amplitude of oscillation in q space, as obtained by numerical solution of Eq. (A1). These considerations explain also why we did not take data for values of q close to the band edges for which dynamics due to the harmonic confinement was not bounded.

[1] F. Bloch, Z. Phys. **52**, 555 (1929); C. Zener, Proc. R. Soc. London, Ser. A **145**, 523 (1934).

[2] M. Raizen, C. Salomon, and Q. Niu, Phys. Today **50**(1), 30 (1997), and references therein.

[3] G. Roati, E. de Mirandes, F. Ferlaino, H. Ott, G. Modugno, and M. Inguscio, Phys. Rev. Lett. **92**, 230402 (2004).

[4] J. Hecker Denschlag, J. E. Simsarian, H. Häffner, C. McKenzie, A. Browaeys, D. Cho, K. Helmerson, S. L. Rolston, and W. D. Phillips, J. Phys. B **35**, 3095 (2002).

[5] L. Fallani, F. S. Cataliotti, J. Catani, C. Fort, M. Modugno, M. Zawada, and M. Inguscio, Phys. Rev. Lett. **91**, 240405 (2003).

[6] B. Eiermann, P. Treutlein, Th. Anker, M. Albiez, M. Taglieber, K.-P. Marzlin, and M. K. Oberthaler, Phys. Rev. Lett. **91**, 060402 (2003).

[7] O. Morsch, J. H. Müller, M. Cristiani, D. Ciampini, and E. Arimondo, Phys. Rev. Lett. **87**, 140402 (2001).

[8] M. Greiner, O. Mandel, T. Esslinger, T. W. Hänsch, and I. Bloch, Nature (London) **415**, 39 (2002).

[9] B. Eiermann, Th. Anker, M. Albiez, M. Taglieber, P. Treutlein, K.-P. Marzlin, and M. K. Oberthaler, Phys. Rev. Lett. **92**, 230401 (2004).

[10] S. Burger, F. S. Cataliotti, C. Fort, F. Minardi, M. Inguscio, M. L. Chiofalo, and M. P. Tosi, Phys. Rev. Lett. **86**, 4447 (2001); B. Wu and Q. Niu, *ibid.* **89**, 088901 (2002); S. Burger, F. S. Cataliotti, C. Fort, F. Minardi, M. Inguscio, M. L. Chiofalo, and M. P. Tosi, *ibid.* **89**, 088902 (2002).

[11] F. S. Cataliotti, L. Fallani, F. Ferlaino, C. Fort, P. Maddaloni, and M. Inguscio, New J. Phys. **5**, 71 (2003).

[12] M. Cristiani, O. Morsch, N. Malossi, M. Jona-Lasinio, M. Anderlini, E. Courtade, and E. Arimondo, Opt. Express **12**, 4 (2004).

[13] L. Fallani, L. De Sarlo, J. E. Lye, M. Modugno, R. Saers, C. Fort, and M. Inguscio, Phys. Rev. Lett. **93**, 140406 (2004).

[14] B. Wu and Q. Niu, Phys. Rev. A **64**, 061603(R) (2001); New J. Phys. **5**, 104 (2003).

[15] A. Smerzi, A. Trombettoni, P. G. Kevrekidis, and A. R. Bishop, Phys. Rev. Lett. **89**, 170402 (2002); C. Menotti, A. Smerzi, and A. Trombettoni, New J. Phys. **5**, 112 (2003).

[16] M. Machholm, C. J. Pethick, and H. Smith, Phys. Rev. A **67**, 053613 (2003); M. Machholm, A. Nicolin, C. J. Pethick, and H. Smith, *ibid.* **69**, 043604 (2004).

[17] F. Kh. Abdullaev, B. B. Baizakov, S. A. Darmanyan, V. V. Konotop, and M. Salerno, Phys. Rev. A **64**, 043606 (2001); V. V. Konotop, and M. Salerno, *ibid.* **65**, 021602(R) (2002).

[18] R. G. Scott, A. M. Martin, T. M. Fromhold, S. Bujkiewicz, F. W. Sheard, and M. Leadbeater, Phys. Rev. Lett. **90**, 110404 (2003).

[19] Y. Zheng, M. Kostrun, and J. Javanainen, Phys. Rev. Lett. **93**, 230401 (2004).

[20] F. Nesi and M. Modugno, J. Phys. B **37**, S101 (2004).

[21] M. Modugno, C. Tozzo, and F. Dalfovo, Phys. Rev. A **70**, 043625 (2004); **71**, 019904(E) (2005).

[22] B. T. Seaman, L. D. Carr, and M. J. Holland, e-print cond-mat/0410347.

[23] See, for example, L. D. Landau and E. M. Lifshitz, *Statistical Physics* (Pergamon Press, Oxford, 1969).

[24] C. Raman, M. Köhl, R. Onofrio, D. S. Durfee, C. E. Kuklewicz, Z. Hadzibabic, and W. Ketterle, Phys. Rev. Lett. **83**, 2502 (1999).

[25] E. Peik, M. Ben Dahan, I. Bouchoule, Y. Castin, and C. Salomon, Phys. Rev. A **55**, 2989 (1997).

[26] M. Krämer, C. Menotti, and M. Modugno, e-print cond-mat/0407014.

[27] E. A. Cornell, J. R. Ensher, and C. E. Wieman, in , Bose-Einstein Condensation in Atomic Gases, Proceedings of the International School of Physics "Enrico Fermi," Course CXL, edited by M. Inguscio, S. Stringari, and C. E. Wieman (IOS Press, Amsterdam, 1999).

[28] P. Pedri, L. Pitaevskii, S. Stringari, C. Fort, S. Burger, F. S. Cataliotti, P. Maddaloni, F. Minardi, and M. Inguscio, Phys. Rev. Lett. **87**, 220401 (2001).

[29] C. Menotti, A. Smerzi, and A. Trombettoni, New J. Phys. **5**, 112 (2003).

[30] S. Dettmer, D. Hellweg, P. Ryytty, J. J. Arlt, W. Ertmer, K. Sengstock, D. S. Petrov, G. V. Shlyapnikov, H. Kreutzmann, L. Santos, and M. Lewenstein, Phys. Rev. Lett. **87**, 160406 (2001); S. Richard, F. Gerbier, J. H. Thywissen, M. Hugbart, P. Bouyer, and A. Aspect, *ibid.* **91**, 010405 (2003).

[31] Y. Castin and R. Dum, Phys. Rev. Lett. **79**, 3553 (1997); Phys. Rev. A **57**, 3008 (1998).

[32] S. A. Gardiner, D. Jaksch, R. Dum, J. I. Cirac, and P. Zoller, Phys. Rev. A **62**, 023612 (2000).

[33] We note that energetic instability, albeit slower than dynamical instability, is still present and so a thermal fraction is unavoidable in the experiment.

[34] N. W. Ashcroft and N. D. Mermin, *Solid State Physics* (Saunders College, Philadelpia, 1976).